Effect of strain on phonons in Si, Ge, and Si/Ge heterostructures

Zhifeng Sui and Irving P. Herman
Department of Applied Physics and the Microelectronics Sciences Laboratories, Columbia University, New York, New York 10027
(Received 27 May 1993)

The dispersion relations for optical and acoustic phonons are examined in bulk Si and Ge, Si and Ge strained layers grown on (001) and (111) surfaces, and ultrathin Si/Ge superlattices at ambient pressure and under hydrostatic pressure by using a modified Keating model. This model includes four interactions, which involve up to the fifth-nearest-neighbor atom, and force constants that depend on strain. These strain-modified force constants are related to specific cubic anharmonic terms in the potential energy and also to the empirical parameters p, q, and r that have been used to describe zone-center phonon shifts and splittings arising from strain. This model is used to obtain the mode Grüneisen parameters γ_i throughout the Brillouin zone for bulk c-Si and c-Ge, and explicit analytic expressions for γ_i at the zone center and boundaries. Biaxial strain in the (001) plane is shown to affect phonon dispersion very differently than in previous work that used a much simpler model. For Si and Ge grown on a (111) substrate, the frequency shift due to the biaxial strain for the TO-phonon mode is found to be almost independent of wave vector. The pressure-induced change in the frequency of confined LO phonons in a $Si_{12}Ge_4$ superlattice predicted by the model agrees with the change measured previously by Raman scattering. This modified Keating model is also used to obtain the second- and third-order elastic constants for Si and Ge.

I. INTRODUCTION

Many Si/Ge/$Si_{1-x}Ge_x$ heterostructures have been grown recently with very high crystallinity despite their large lattice mismatches of up to 4.2%.[1,2] There have been extensive efforts to understand the electronic and lattice properties of these and other artificially grown materials, which are known to depend critically on the effects of biaxial strain and confinement.[3,4] The application of both hydrostatic pressure and uniaxial stress are very useful in understanding these properties and in altering them. For example, the biaxial strain in these strained-layer heterostructures can be tuned by applying pressure, and this change can be monitored by its effect on electronic and phonon properties. Such strain-related changes in phonon frequencies in Si/Ge strained-layer superlattices (SLS's) have been investigated by Raman scattering by our group.[5] In the present work, the effect of strain on phonons in Si/Ge heterostructures and in bulk Si and Ge is investigated by using a modified Keating model[6–8] that is sufficiently comprehensive to relate and explain all available data, yet simple enough to determine details of the lattice dynamics without resorting to *ab initio* methods. The strain may arise from the growth conditions or from the application of external stress.

The dispersion relations of optical and acoustic phonons at ambient pressure and the mode Grüneisen parameters γ_i are obtained in bulk Si and Ge throughout the Brillouin zone. Explicit analytic expressions for γ_i at the zone center and boundaries are presented. Phonon dispersion is also studied in strained Si and Ge films at ambient pressure and at elevated pressure. The empirical parameters p, q, and r that have often been used to relate zone-center phonon shifts and splittings due to strain[8] are expressed in terms of model parameters. Analytic expressions for second-order and third-order elastic constants are also derived with this model.

The dispersion relations for phonons in strained Si and Ge have been calculated by several groups. For example, Gianozzi *et al.*[9] and Qteish and Molinari[10] recently used an *ab initio* approach based on density-functional theory in the local-density approximation to investigate lattice dynamics in isotropically and biaxially strained structures. Using a much simpler, but less fundamental approach, Zi, Zhang, and Xie[7] examined phonon dispersion in biaxially strained Si and Ge (001) layers and in Si/Ge SLS's by using a Keating model with strain-modified force constants. They added strain-induced perturbations to the two Keating parameters for bond bending and stretching, as had been suggested earlier by Cerdeira *et al.*[8] Ghanbari *et al.*[11] used a modified version of the valence-force-field model with six parameters to describe phonon dispersion in Si/Ge SLS's. They adopted strain-perturbed force constants that scale as a power of the interatomic distance for the interactions relating to bond stretching, but used different scaling parameters for transverse and longitudinal modes. However, they assumed that the angular dependence of the force constants is not affected by strain. Although the models in Refs. 7, 8, and 11 were fit to some of the available experimental data, they do not produce the correct dispersion of the mode Grüneisen parameter $\gamma_i = -d\ln\omega_i / d\ln V$, which characterizes the effect of isotropic strain on the phonon frequency ω_i for mode i; V is the volume.

In early lattice-dynamic calculations, Dolling and Cowley[12] and Jex[13] determined the dispersion of the mode Grüneisen parameters γ_i in Si and Ge by adjusting nearest-neighbor[12,13] and next-nearest-neighbor[13] anhar-

monic terms to fit the temperature dependence of the thermal conductivity. Though their results are qualitatively reasonable for TO, LO, and LA phonons, they are poor for TA phonons. More recently, Xu *et al.*[14] determined the dispersion of γ_i in Si by using a tight-binding calculation to obtain the force-constant matrix. However, optical-phonon frequencies were overestimated by $\sim 10\%$ in that study. Recent *ab initio* calculations[15] have obtained γ_i for *c*-Si and *c*-Ge that are in excellent agreement with experimental data.

The Keating model is known to give a good description of LO, TO, and LA modes in unstrained covalent semiconductors, but it does not reproduce the flatness of the TA mode dispersion.[16] More complex lattice-dynamics models, such as the six-parameter valence-force-field (VFF) potential method[17,18] and the four-parameter adiabatic bond charge model,[16] describe all Si and Ge modes quite well.

In the present work, a modified Keating/VFF model is used, which includes four types of interactions—the original Keating bond-stretching and bond-bending interactions, and also the nearest-bond and nearest-coplanar-angle interactions. This model is presented in Sec. II A, and in Sec. II B it is shown to give the correct phonon dispersion for unstrained Si and Ge at ambient pressure. In Sec. II C, strain-modified force constants are introduced and treated as model parameters that are determined by fitting available mode Grüneisen parameter data at the zone center and boundaries. The mode Grüneisen parameters are determined along the [001] and [111] directions in bulk Si and Ge. The effect of biaxial strain in the (001) plane on phonons is discussed in Sec. II D. This is continued for strain in the (111) plane in Sec. II E. The effect of pressure on phonons is strained Si and Ge layers and Si/Ge superlattices grown in the [001] and [111] directions is investigated in Sec. II F. The empirical parameters p, q, and r that have been used to relate zone-center phonon shifts and splittings due to strain are expressed in terms of model parameters in Sec. III.

The use of strain-modified force constants is justified in Sec. IV by examining lattice dynamics with cubic terms added to the Hamiltonian and determining quasiharmonic force constants. The use of this model for obtaining elastic constants is discussed in Sec. V, where the third-order elastic constants are derived. A general discussion of the results is presented in Sec. VI, which is followed by concluding remarks in Sec. VII.

II. MODEL

A. General formalism

The potential energy used by Keating[19] takes into account only the bond-stretching and bond-bending interactions. Although it describes optical phonons fairly well, it gives a very poor description of the TA-phonon dispersion, where the predicted phonon frequency is $\sim 80\%$ too high at the X and L points. Consequently, further interactions with neighboring atoms are needed. While as many as six harmonic interactions have been included in modeling Si and Ge,[17,18] it is found here that only four interactions are needed to describe the dispersion well. The other two interactions give relatively small contributions. The potential energy is

$$U=\tfrac{1}{2}\sum_{l}\sum_{i=1}^{4}\alpha\Delta r\begin{bmatrix}l\\i\end{bmatrix}\Delta r\begin{bmatrix}l\\i\end{bmatrix}+\frac{1}{2}\sum_{l}\sum_{ji}\beta\Delta\theta\begin{bmatrix}l\\ij\end{bmatrix}\Delta\theta\begin{bmatrix}l\\ij\end{bmatrix}+\tfrac{1}{2}\sum_{ll'}\sum_{jin}\kappa\Delta\theta\begin{bmatrix}l\\ij\end{bmatrix}\Delta\theta\begin{bmatrix}l'\\jn\end{bmatrix}+\tfrac{1}{2}\sum_{ll'}\sum_{ji}\tau\Delta r\begin{bmatrix}l\\i\end{bmatrix}\Delta r\begin{bmatrix}l'\\j\end{bmatrix}. \quad (1)$$

$\Delta r\binom{l}{i}$ and $\Delta\theta\binom{l}{ij}$ are defined as

$$\Delta r\begin{bmatrix}l\\i\end{bmatrix}=\frac{\mathbf{r}\begin{bmatrix}l\\i\end{bmatrix}\cdot\Delta\tilde{\mathbf{u}}\begin{bmatrix}l\\i\end{bmatrix}}{a'}, \quad (2a)$$

$$\Delta\theta\begin{bmatrix}l\\ij\end{bmatrix}=\frac{1}{2a'}\left\{\mathbf{r}\begin{bmatrix}l\\i\end{bmatrix}\cdot\Delta\tilde{\mathbf{u}}\begin{bmatrix}l\\j\end{bmatrix}+\mathbf{r}\begin{bmatrix}l\\j\end{bmatrix}\cdot\Delta\tilde{\mathbf{u}}\begin{bmatrix}l\\i\end{bmatrix}\right\}, \quad (2b)$$

where $a'=a_0/4$, and a_0 is the lattice constant. $\mathbf{r}\binom{l}{i}$ is the ith bond vector in the lth primitive cell at ambient conditions and $\Delta\tilde{\mathbf{u}}\binom{l}{i}$ is the relative displacement of the ith bond vector in the lth primitive cell.

$\Delta r\binom{l}{i}$ and $\Delta\theta\binom{l}{ij}$ are the valence coordinates associated with bond stretching and bond bending, respectively, labeled by the bonds that are involved. They are also scalars so that the potential energy defined in Eq. (1) is rotationally invariant. In later sections it will sometimes be clearer to label Δr by the two atoms involved in the bond, such as $\Delta r\binom{0\ 1}{\beta\ \eta}$, and $\Delta\theta$ by the three atoms involved, such as $\Delta\theta\binom{0\ 0\ 1}{\eta\ \beta\ \eta}$ (see Fig. 1 and also Ref. 18). Equations (2a) and (2b) give the relations between the valence coordinates and the first-order displacements of the atoms, which are derived from Keating's original coordinates by neglecting higher-order terms. The coefficients in Eqs. (2a) and (2b) determine the transformation matrix that connects valence coordinates to Cartesian coordinates.

The first summation in Eq. (1) describes bond stretching and compression with force constant α; there are four bonds labeled with $i=1$ to 4 in each primitive cell, and l is the cell index. The second term characterizes the bond-bending interaction with force constant β, and the indices i and j are associated with the bond i and bond j that share a common apex; there are 12 angles that contribute to this interaction in each primitive cell. The third term describes the nearest angle-angle interaction, with force constant κ, which is between two nearest coplanar angles that share one common bond with different apices, as described in Ref. 18. The fourth term describes the bond-bond interactions, with force constant τ between two nearest bonds sharing a common apex; there are 12 terms for each cell. Figure 2 illustrates these four

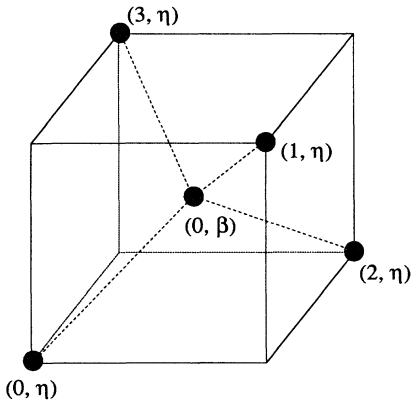

FIG. 1. Diamond crystal structure. The bonds shown belong to the unit cell labeled 0 containing atoms $(0,\eta)$ and $(0,\beta)$.

harmonic interactions. The two harmonic terms from Ref. 18 that are neglected here are the interactions between a bond and an angle sharing one common bond and that between two nearest nonplanar angles.

$\Delta\tilde{\mathbf{u}}\begin{pmatrix} l \\ i \end{pmatrix}$ has contributions due to dynamic displacement and static strain displacement. In linear approximation

$$\Delta\tilde{\mathbf{u}}\begin{pmatrix} l \\ i \end{pmatrix}=\Delta\mathbf{u}_d\begin{pmatrix} l \\ i \end{pmatrix}+\Delta\mathbf{u}_s\begin{pmatrix} l \\ i \end{pmatrix}, \tag{3}$$

where $\Delta\mathbf{u}_d(\begin{smallmatrix} l \\ i \end{smallmatrix})$ is the relative dynamic displacement of two atoms attached by the ith bond in the lth cell and $\Delta\mathbf{u}_s(\begin{smallmatrix} l \\ i \end{smallmatrix})$ is the static displacement between two neighboring atoms under external strain, which is

$$\Delta\mathbf{u}_s\begin{pmatrix} l \\ i \end{pmatrix}=\overleftrightarrow{\varepsilon}\,\mathbf{r}\begin{pmatrix} l \\ i \end{pmatrix}-a'\xi\begin{pmatrix} e_{yz} \\ e_{xz} \\ e_{xy} \end{pmatrix}. \tag{4}$$

ξ is the internal strain parameter and $\overleftrightarrow{\varepsilon}$ is the deformation tensor, whose components ε_{ij} are related to the strain tensor elements e_{ij} by

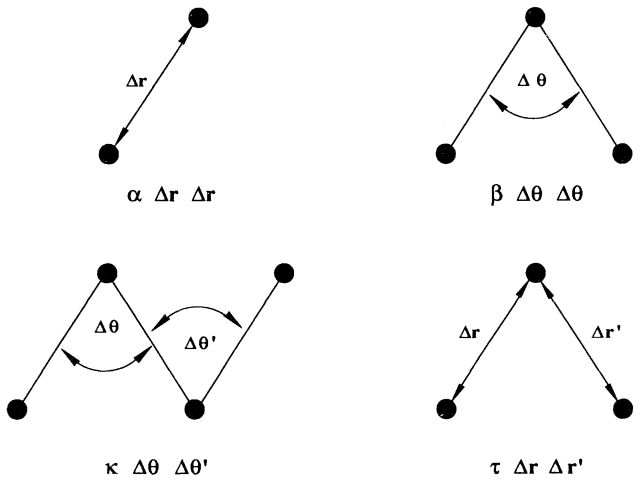

FIG. 2. Schematic representation of the harmonic interactions in Eq. (1).

$$\begin{aligned} &e_{xx}=\varepsilon_{xx},\quad e_{yy}=\varepsilon_{yy},\quad e_{zz}=\varepsilon_{zz},\\ &e_{xy}=\varepsilon_{xy}+\varepsilon_{yx},\quad e_{xz}=\varepsilon_{xz}+\varepsilon_{zx},\quad e_{yz}=\varepsilon_{yz}+\varepsilon_{zy}. \end{aligned} \tag{5}$$

Inserting Eqs. (2a), (2b), and (3) into Eq. (1), the potential energy can be expressed as

$$U=U_0+U_1+U_2\ . \tag{6}$$

U_0 contains quadratic static strain contributions, and has the same form as Eq. (1) with $\Delta\tilde{\mathbf{u}}(\begin{smallmatrix} l \\ i \end{smallmatrix})$ replaced by $\Delta\mathbf{u}_s(\begin{smallmatrix} l \\ i \end{smallmatrix})$. U_1 contains cross terms, such as $\Delta\mathbf{u}_s(\begin{smallmatrix} l \\ i \end{smallmatrix})\Delta\mathbf{u}_d(\begin{smallmatrix} l \\ j \end{smallmatrix})$, and vanishes because of the absence of the net exerted force. U_2 is the summation of terms quadratic in $\Delta\mathbf{u}_d(\begin{smallmatrix} l \\ i \end{smallmatrix})$, and has the same form as Eq. (1) with $\Delta\tilde{\mathbf{u}}(\begin{smallmatrix} l \\ i \end{smallmatrix})$ replaced by $\Delta\mathbf{u}_d(\begin{smallmatrix} l \\ i \end{smallmatrix})$.

Keating[19] included only the first two terms in Eq. (1). Moreover, he defined

$$\Delta r\begin{pmatrix} l \\ i \end{pmatrix}=\frac{1}{2a'}\left\{2\mathbf{r}\begin{pmatrix} l \\ i \end{pmatrix}\cdot\Delta\tilde{\mathbf{u}}\begin{pmatrix} l \\ i \end{pmatrix}+\Delta\tilde{\mathbf{u}}\begin{pmatrix} l \\ i \end{pmatrix}\cdot\Delta\tilde{\mathbf{u}}\begin{pmatrix} l \\ i \end{pmatrix}\right\}, \tag{7a}$$

$$\begin{aligned}\Delta\theta\begin{pmatrix} l \\ ij \end{pmatrix}=\frac{1}{2a'}&\left\{\mathbf{r}\begin{pmatrix} l \\ i \end{pmatrix}\cdot\Delta\tilde{\mathbf{u}}\begin{pmatrix} l \\ j \end{pmatrix}+\mathbf{r}\begin{pmatrix} l \\ j \end{pmatrix}\cdot\Delta\tilde{\mathbf{u}}\begin{pmatrix} l \\ i \end{pmatrix}\right.\\ &\left.+\Delta\tilde{\mathbf{u}}\begin{pmatrix} l \\ i \end{pmatrix}\cdot\Delta\tilde{\mathbf{u}}\begin{pmatrix} l \\ j \end{pmatrix}\right\}, \end{aligned} \tag{7b}$$

instead of as in Eqs. (2a) and (2b). The second term on the right side in Eq. (7a) and the third term in Eq. (7b) can be ignored because they are second-order quantities. Both definitions [Eqs. (2) and (7)] are rotationally invariant and equivalent up to first order in displacement.

The static and dynamic strain contributions are cleanly separated in the current approach. U_0 describes the effect of static strain as characterized by the second-order elastic constants, while U_2 describes phonons. Strain was included in the previous studies that used two Keating interactions[7,8] by replacing $\mathbf{r}(\begin{smallmatrix} l \\ i \end{smallmatrix})$ by $\mathbf{r}(\begin{smallmatrix} l \\ i \end{smallmatrix})+\Delta\mathbf{u}_s(\begin{smallmatrix} l \\ i \end{smallmatrix})$ and $\Delta\tilde{\mathbf{u}}(\begin{smallmatrix} l \\ i \end{smallmatrix})$ by $\Delta\mathbf{u}_d(\begin{smallmatrix} l \\ i \end{smallmatrix})$ in Eqs. (2a) and (2b), which does not lead to the separation of the static and dynamic terms, as in Eq. (6). Consequently, a' depends on static strain in this earlier work. The two approaches give the same analytical results, but the parameters have different physical meanings.

Anharmonic interactions are included by using quasiharmonic force constants α, β, κ, and τ that depend on the strain in the harmonic potential energy U_2. Following Refs. 7 and 8, these quasiharmonic force constants have the following form:

$$\alpha_i=\alpha_0\left[1+n_\alpha\frac{\Delta r_i}{r_0}\right], \tag{8a}$$

$$\beta_{ij}=\beta_0\left[1+m_\beta\frac{\Delta(r_ir_j)}{2r_0^2}+l_\beta\frac{\Delta\cos\theta_{ij}}{\cos\theta_0}\right], \tag{8b}$$

$$\begin{aligned}\kappa_{ijk}=\kappa_0&\left\{1+m_\kappa\left[\frac{\Delta(r_ir_j)}{4r_0^2}+\frac{\Delta(r_jr_k)}{4r_0^2}\right]\right.\\ &\left.+l_\kappa\frac{\Delta(\cos\theta_{ij}\cos\theta_{jk})}{2\cos^2\theta_0}\right\}, \end{aligned} \tag{8c}$$

$$\tau_{ij}=\tau_0\left[1+n_\tau\frac{\Delta(r_ir_j)}{2r_0^2}+l_\tau\frac{\Delta\cos\theta_{ij}}{\cos\theta_0}\right], \tag{8d}$$

where the parameters with index 0 are those for no strain ($r_0=\sqrt{3}a'$, $\cos\theta_0=-\frac{1}{3}$), r_i is the ith bond length, and θ_{ij} is the angle between the ith and the jth bond. The use of quasiharmonic force constants will be justified in Sec. IV.

B. Ambient pressure

The second-order macroscopic strain energy density for cubic crystals is[19]

$$\frac{U_0}{V}=\tfrac{1}{2}C_{11}(e_{xx}^2+e_{yy}^2+e_{zz}^2)+C_{12}(e_{xx}e_{yy}+e_{xx}e_{zz}+e_{yy}e_{zz})+\tfrac{1}{2}C_{44}(e_{xy}^2+e_{xz}^2+e_{yz}^2)\ , \tag{9}$$

where V is the volume of the crystal and C_{11}, C_{12}, and C_{44} are the second-order elastic constants. Comparing the potential energy U_0 in Eq. (6) with the macroscopic energy density in Eq. (9) gives

$$C_{11}=\frac{1}{4a'}(\alpha+3\beta+3\kappa+3\tau)\ , \tag{10a}$$

$$C_{12}=\frac{1}{4a'}(\alpha-\beta-\kappa+3\tau)\ , \tag{10b}$$

$$C_{44}=\frac{1}{4a'}[(1-\xi)^2\alpha+(1+\xi)^2\beta+(1+\xi)^2\kappa-\tau]\ . \tag{10c}$$

The bulk modulus is

$$B=\frac{C_{11}+2C_{12}}{3}=\frac{1}{12a'}(3\alpha+\beta+\kappa+9\tau)\ . \tag{10d}$$

The static strain energy U_0 is minimized by setting $dU_0/d\xi=0$, which gives

$$\xi=\frac{\alpha-\beta-\kappa-\tau}{\alpha+\beta+\kappa-\tau}\ . \tag{10e}$$

When only α and β are assumed to be nonzero, Eqs. (10a)–(10e) reduce to the expressions in Ref. 19.

Phonon dispersion is determined by converting U_2 to Cartesian coordinates, adding it to the kinetic energy, and performing normal mode analysis, as in Ref. 18. This leads to analytic expressions for phonon frequencies at the center and boundaries of the Brillouin zone, which are tabulated in Table I. The four parameters for zero strain, α_0, β_0, κ_0, and τ_0, have been optimized by using neutron-scattering data along the [001] and [111] directions,[20,21] and are listed in Table II for Si and Ge. Phonon dispersion is plotted in Fig. 3 for Si and Fig. 4 for Ge. The fits are much better for all phonon branches *vis-à-vis* those using only two parameters (α_0,β_0), especially for TA phonons. The average deviation of phonon frequencies is 1.7% for Si and 2.3% for Ge with this four-parameter model.

C. Hydrostatic pressure

The crystal symmetry remains the same under hydrostatic pressure, and therefore there are no changes in bond angles ($\Delta\cos\theta=0$). The bond lengths are uniformly compressed, and the quasiharmonic force constants change accordingly. The hydrostatic strain is

$$e_{xx}=e_{yy}=e_{zz} \quad \text{and} \quad e_{xy}=e_{xz}=e_{yz}=0\ . \tag{11}$$

The change in bond length is $\Delta r=r_0e_{xx}$. By using Eqs. (8a)–(8d), the strain-modified force constants are

$$\alpha=\alpha_0(1+n_\alpha e_{xx})\ , \tag{12a}$$

$$\beta=\beta_0(1+m_\beta e_{xx})\ , \tag{12b}$$

$$\kappa=\kappa_0(1+m_\kappa e_{xx})\ , \tag{12c}$$

$$\tau=\tau_0(1+n_\tau e_{xx})\ , \tag{12d}$$

where n_α, m_β, m_κ, and n_τ characterize how the force constants depend on hydrostatic strain.

The change in bond length under hydrostatic pressure is

TABLE I. The phonon frequencies obtained from the model at the Γ, X, and L points for different modes, where M is the mass of the Si or Ge atom. The corresponding experimental values are listed in parentheses for Si at 300 K (Ref. 20) and for Ge at 80 K (Ref. 21).

		Si (cm^{-1})	Ge (cm^{-1})
$\omega_{LO,TO}(\Gamma)$	$\left[\frac{8(\alpha+\beta+\kappa-\tau)}{M}\right]^{1/2}$	518.4 (520.5)	302.2 (304)
$\omega_{LO,LA}(X)$	$\left[\frac{4(\alpha+2\beta+\kappa+\tau)}{M}\right]^{1/2}$	413.3 (411)	241.5 (240)
$\omega_{TO}(X)$	$\left[\frac{8(\alpha-\tau)}{M}\right]^{1/2}$	460.6 (463)	270.4 (275)
$\omega_{TA}(X)$	$\left[\frac{8\beta}{M}\right]^{1/2}$	151.6 (150)	82.7 (80.0)
$\omega_{LO}(L)$	$\left[\frac{6\alpha+\beta}{M}\right]^{1/2}$	425.1 (420)	250.2 (245)
$\omega_{TO}(L)$	$\left[\frac{8\alpha+4\beta+4\kappa-8\tau}{M}\right]^{1/2}$	490.4 (489)	286.8 (290)
$\omega_{LA}(L)$	$\left[\frac{2\alpha+13\beta+4\kappa+4\tau}{M}\right]^{1/2}$	354.8 (378)	205.9 (222)
$\omega_{TA}(L)$	$\left[\frac{4\beta}{M}\right]^{1/2}$	107.2 (114)	58.5 (63.3)

TABLE II. Parameters used in the modified Keating model, fit to the phonon data only.

	Si	Ge	unit
α_0	4.940	4.432	10^4 dyn/cm
β_0	0.479	0.368	10^4 dyn/cm
κ_0	0.699	0.613	10^4 dyn/cm
τ_0	0.520	0.495	10^4 dyn/cm
n_α	−9.58	−9.71	
n_τ	−14.5	−15.9	
m_β	8.40	9.18	
m_κ	4.07	5.70	
l_β	7.36	4.91	
l_κ	−5.25	−3.80	
l_τ	−1.39	−0.28	

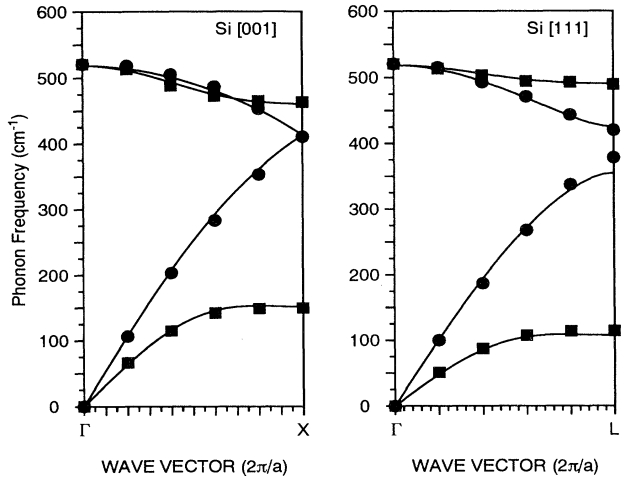

FIG. 3. Phonon-dispersion relations along [001] and [111] in Si. The solid circles and solid squares are the neutron-scattering data (Ref. 20) for longitudinal and transverse phonons, respectively.

$$\frac{\Delta r}{r_0}=-\frac{P}{3B}\ , \tag{13}$$

where P is the applied pressure. Analytic expressions for the mode Grüneisen parameters γ_i at the Γ, X, and L points are obtained by using the expressions in Table I, Eqs. (12a)–(12d) and

$$\gamma_i=-\frac{d\ln\omega_i}{d\ln V}=\frac{B}{\omega_i}\frac{d\omega_i}{dP}\ , \tag{14}$$

where ω_i is the phonon frequency of mode i. They are listed in Table III.

n_α, m_β, m_κ, and n_τ were determined by fitting the values of the Grüneisen parameter for optical phonons. Specifically, for Si

$$\gamma_{\mathrm{LO,TO}}(\Gamma)=-\frac{n_\alpha\alpha_0+m_\beta\beta_0+m_\kappa\kappa_0-n_\tau\tau_0}{6(\alpha_0+\beta_0+\kappa_0-\tau_0)}=0.98\ , \tag{15a}$$

$$\gamma_{\mathrm{TO}}(X)=-\frac{n_\alpha\alpha_0-n_\tau\tau_0}{6(\alpha_0-\tau_0)}=1.5\ , \tag{15b}$$

$$\gamma_{\mathrm{TA}}(X)=-\frac{m_\beta}{6}=-1.4\ , \tag{15c}$$

$$\gamma_{\mathrm{LO,LA}}(X)=-\frac{n_\alpha\alpha_0+2m_\beta\beta_0+m_\kappa\kappa_0+n_\tau\tau_0}{6(\alpha_0+2\beta_0+\kappa_0+\tau_0)}=1.03\ . \tag{15d}$$

The numerical values for γ_i in Eqs. (15a)–(15c) were obtained from Raman scattering,[22] while that in Eq. (15d) was taken from the *ab initio* calculation in Ref. 15, which generally agrees well with experimental data. The four model parameters so determined are listed in Table II.

Reference 7 assumed that $n_\alpha=m_\beta$ in their calculation of the dispersion of ω under biaxial strain; this assumption had been suggested earlier in Ref. 8. Both studies utilized only the two Keating interactions parametrized by α and β, and the current parameters n_α and m_β, labeled as n and m in Ref. 7, to describe isotropic strain. This assumption of equal n_α and m_β implies that $\gamma=-n_\alpha/6=-m_\beta/6$ for LO, TO, TA, and LA phonons at each symmetry point (Table III) and, in fact, throughout the Brillouin zone. Consequently, it gives the incorrect dispersion of γ for each branch. This assumption is expected to lead to errors in describing how biaxial strain affects phonon frequencies away from zone center.

The current model gives $\gamma_{\mathrm{TA}}(X)=-m_\beta/6$. Since $\gamma_{\mathrm{TA}}(X)$ is known to be negative in c-Si and c-Ge,[22,23] which is consistent with the anomalous thermal expansion at low temperatures, m_β would be expected to be positive. This suggests that bond compression decreases the energy for angular interactions, which is in contrast to earlier expectations.[7,8]

The fits for Ge are less strongly based on experiment than those for Si. In Ge, apparently only $\gamma_{\mathrm{LO,TO}}(\Gamma)$ and $\gamma_{\mathrm{TA}}(X)$ have been measured by Raman scattering.[23] $\gamma_{\mathrm{LO,TO}}(\Gamma)=0.96$ is used here, which is obtained by using $d\omega(\Gamma)/dP=0.385$ cm^{-1}kbar^{-1} in Ref. 23 and the second expression for γ_i in Eq. (14). Early L-point measurements of other γ_i in Ge by tunneling[24] are questionable. $\gamma_{\mathrm{TO}}(X)=1.49$ is used from *ab initio* calculations,[15] which also show that $\gamma_{\mathrm{LO,LA}}(X)$ is greater than $\gamma_{\mathrm{LO,TO}}(\Gamma)$ by 0.12. Assuming this difference is accurate, $\gamma_{\mathrm{LO,LA}}(X)=1.08$.

The mode Grüneisen parameters for Si and Ge along [001] and [111] were determined by calculating the difference between ω at ambient pressure and at a low pressure, using our values for n_α, m_β, m_κ, and n_τ (Table II). They are plotted in Figs. 5 and 6, and are in qualitative agreement with the previous calculations along Δ and Λ in Ref. 15 using the *ab initio* calculations for c-Si

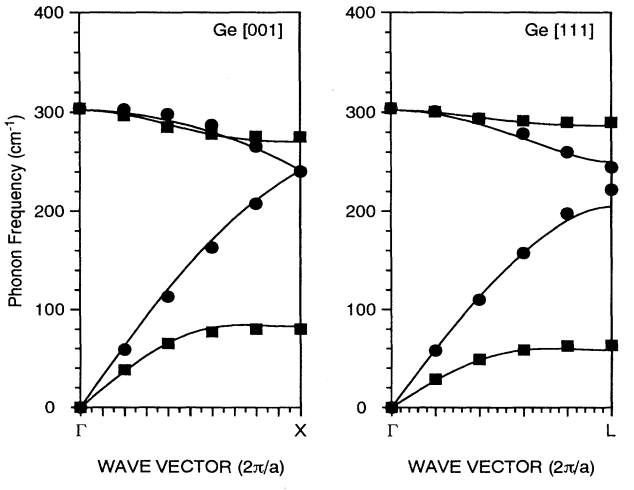

FIG. 4. Phonon-dispersion relations along [001] and [111] in Ge. The solid circles and solid squares are the neutron-scattering data (Ref. 21) for longitudinal and transverse phonons, respectively.

TABLE III. The Grüneisen parameters obtained from available experimental data for Si and Ge. The values in parentheses are from the *ab initio* calculation in Ref. 15.

	Theoretical	Si	Ge
$\gamma_{\mathrm{LO,TO}}(\Gamma)$	$-\frac{n_\alpha\alpha_0+m_\beta\beta_0+m_\kappa\kappa_0-n_\tau\tau_0}{6(\alpha_0+\beta_0+\kappa_0-\tau_0)}$	0.98±0.06[a] (0.99)	0.96±0.05[b] (1.05)
$\gamma_{\mathrm{LO,LA}}(X)$	$-\frac{n_\alpha\alpha_0+2m_\beta\beta_0+m_\kappa\kappa_0+n_\tau\tau_0}{6(\alpha_0+2\beta_0+\kappa_0+\tau_0)}$	(1.03)	(1.17)
$\gamma_{\mathrm{TO}}(X)$	$-\frac{n_\alpha\alpha_0-n_\tau\tau_0}{6(\alpha_0-\tau_0)}$	1.5±0.2[a] (1.50)	(1.49)
$\gamma_{\mathrm{TA}}(X)$	$-\frac{m_\beta}{6}$	−1.4±0.3[a] (−1.52)	−1.53±0.1[c] (−1.53)
$\gamma_{\mathrm{LO}}(L)$	$-\frac{6n_\alpha\alpha_0+m_\beta\beta_0}{6(6\alpha_0+\beta_0)}$	(1.62)	(1.67)
$\gamma_{\mathrm{TO}}(L)$	$-\frac{2n_\alpha\alpha_0+m_\beta\beta_0+m_\kappa\kappa_0-2n_\tau\tau_0}{6(2\alpha_0+\beta_0+\kappa_0-2\tau_0)}$	1.3±0.2[a] (1.24)	(1.28)
$\gamma_{\mathrm{LA}}(L)$	$-\frac{2n_\alpha\alpha_0+13m_\beta\beta_0+4m_\kappa\kappa_0+4n_\tau\tau_0}{6(2\alpha_0+13\beta_0+4\kappa_0+4\tau_0)}$	(0.45)	(0.55)
$\gamma_{\mathrm{TA}}(L)$	$-\frac{m_\beta}{6}$	−1.3±0.3[a] (−1.24)	(−1.40)

[a]Measured in Ref. 22.
[b]The $\gamma_{\mathrm{LO}}(\Gamma)$ for Ge is obtained from $\gamma_i=(B/\omega_i)(d\omega_i/dP)$, with $d\omega_i/dP=0.385\ \mathrm{cm}^{-1}\,\mathrm{kbar}^{-1}$, as measured in Ref. 23.
[c]Measured in Ref. 23.

and *c*-Ge, and in Ref. 14 using the tight-binding model for *c*-Si. This is not surprising since much of the data used here agree with (or in some cases actually are) the *ab initio* results.

D. Biaxial strain in the (001) plane

When a very thin film is pseudomorphically grown on a substrate, the in-plane lattice constant of the film is the same as that of the substrate, while the in-plane lattice constant of the substrate is unaffected by the film. This is the prototype strained layer considered in this study. Other types of strain configurations, such as freely standing heterostructures, can be analyzed with only slight modifications.

With biaxial strain in the (001) plane, the elements of the strain tensor in the film are

$$e_{xx}=e_{yy}=\frac{a^s-a^f}{a^f}\ ,\quad e_{zz}=-\frac{2C_{12}}{C_{11}}e_{xx}\ , \tag{16}$$

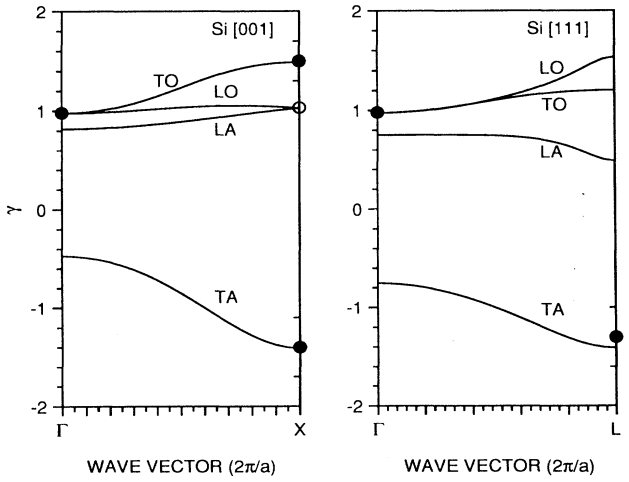

FIG. 5. The mode Grüneisen parameters along [001] and [111] in Si. The solid circles are from Raman-scattering studies (Ref. 22). The open circle is the *ab initio* point from Ref. 15 used in the fit.

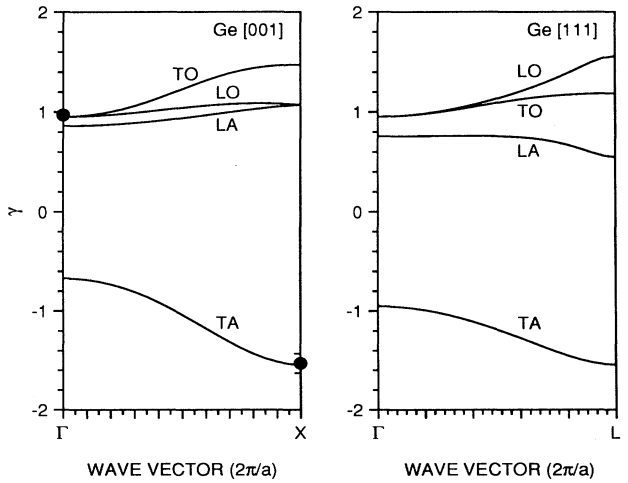

FIG. 6. The mode Grüneisen parameters along [001] and [111] in Ge. The solid circles are from Raman-scattering studies (Ref. 23).

and

$$e_{xy}=e_{xz}=e_{yz}=0 ,$$

where a^f and a^s are the lattice constants for the film and the substrate, respectively. The strain can be decomposed into a hydrostatic strain component

$$e^h_{xx}=e^h_{yy}=e^h_{zz}=\frac{2}{3}\left[1-\frac{C_{12}}{C_{11}}\right]e_{xx} \tag{17a}$$

and a traceless strain component

$$e^b_{xx}=e^b_{yy}=-\tfrac{1}{2}e^b_{zz}=\frac{1}{3}\left[1+\frac{2C_{12}}{C_{11}}\right]e_{xx} , \tag{17b}$$

so $e=e^h+e^b$.

To first order, isotropic strain affects only the bond lengths and the traceless strain components alter only the equilibrium bond angles. With (001) biaxial strain, four bond angles, $\Delta\theta(\begin{smallmatrix}0&0&-3\\ \beta&\eta&\beta\end{smallmatrix})$, $\Delta\theta(\begin{smallmatrix}0&0&3\\ \eta&\beta&\eta\end{smallmatrix})$, $\Delta\theta(\begin{smallmatrix}-1&0&-2\\ \beta&\eta&\beta\end{smallmatrix})$, and $\Delta\theta(\begin{smallmatrix}1&0&2\\ \beta&\eta&\beta\end{smallmatrix})$, change by $2\sqrt{2}e^b_{xx}$ from their ambient equilibrium angles, while the other eight bond angles change by $-\sqrt{2}e^b_{xx}$. Therefore, using Eqs. (8a)–(8d), the quasiharmonic force constants are

$$\alpha=\alpha_0(1+n_\alpha e^h_{xx}) , \tag{18a}$$

$$\beta_1=\beta_0(1+m_\beta e^h_{xx}-4l_\beta e^b_{xx}) , \tag{18b}$$

$$\beta_2=\beta_0(1+m_\beta e^h_{xx}+8l_\beta e^b_{xx}) , \tag{18c}$$

$$\kappa_1=\kappa_0(1+m_\kappa e^h_{xx}-4l_\kappa e^b_{xx}) , \tag{18d}$$

$$\kappa_2=\kappa_0(1+m_\kappa e^h_{xx}+8l_\kappa e^b_{xx}) , \tag{18e}$$

$$\tau_1=\tau_0(1+n_\tau e^h_{xx}-4l_\tau e^b_{xx}) , \tag{18f}$$

$$\tau_2=\tau_0(1+n_\tau e^h_{xx}+8l_\tau e^b_{xx}) , \tag{18g}$$

where l_β, l_κ, and l_τ are the parameters associated with bond-angle changes.

Under biaxial strain, TO- and LO-phonon frequencies at zone center (Γ point) are

$$\omega_{\rm LO}(\Gamma)=\left[\frac{8(\alpha+\beta_2+\kappa_2-\tau_1)}{M}\right]^{1/2} , \tag{19a}$$

$$\omega_{\rm TO}(\Gamma)=\left[\frac{8(\alpha+\beta_1+\kappa_1-\tau_2)}{M}\right]^{1/2} , \tag{19b}$$

where M is the mass of the (Si or Ge) atom. The corresponding shifts in frequency due to biaxial strain are obtained by inserting Eqs. (18a)–(18e) into Eqs. (19a) and (19b), and expanding to first order in strain. Thus,

$$\Delta\omega_{\rm LO}(\Gamma)=\left\{\frac{n_\alpha\alpha_0+m_\beta\beta_0+m_\kappa\kappa_0-n_\tau\tau_0}{3(\alpha_0+\beta_0+\kappa_0-\tau_0)}\left[1-\frac{C_{12}}{C_{11}}\right]+\frac{2}{3}\frac{2l_\beta\beta_0+2l_\kappa\kappa_0+l_\tau\tau_0}{\alpha_0+\beta_0+\kappa_0-\tau_0}\left[1+\frac{2C_{12}}{C_{11}}\right]\right\}e_{xx}\omega_0(\Gamma) , \tag{20a}$$

$$\Delta\omega_{\rm TO}(\Gamma)=\left\{\frac{n_\alpha\alpha_0+m_\beta\beta_0+m_\kappa\kappa_0-n_\tau\tau_0}{3(\alpha_0+\beta_0+\kappa_0-\tau_0)}\left[1-\frac{C_{12}}{C_{11}}\right]-\frac{2}{3}\frac{l_\beta\beta_0+l_\kappa\kappa_0+2l_\tau\tau_0}{\alpha_0+\beta_0+\kappa_0-\tau_0}\left[1+\frac{2C_{12}}{C_{11}}\right]\right\}e_{xx}\omega_0(\Gamma) . \tag{20b}$$

(20b)

The splitting of the TO- and LO-phonon frequencies at zone center is

$$\omega_{\rm LO}(\Gamma)-\omega_{\rm TO}(\Gamma)=\left[\frac{2(l_\beta\beta_0+l_\kappa\kappa_0+l_\tau\tau_0)}{\alpha_0+\beta_0+\kappa_0-\tau_0}\right]\left[1+\frac{2C_{12}}{C_{11}}\right]e_{xx}\omega_0(\Gamma) . \tag{21}$$

In Sec. III it will be seen that the term in the first bracket is the negative of $(p-q)/2\omega_0^2(\Gamma)$, the shear phonon deformation parameter, where p and q are parameters defined in Sec. III and Ref. 8. This deformation parameter has been measured to be 0.31 for Si and 0.23 for Ge.[8]

At the X point, the shift in the LO frequency due to biaxial strain is

$$\begin{aligned}\Delta\omega_{\rm LO}(X)&=\left[\frac{4(\alpha+\beta_1+\beta_2+\kappa_2+\tau_1)}{M}\right]^{1/2}-\left[\frac{4(\alpha_0+2\beta_0+\kappa_0+\tau_0)}{M}\right]^{1/2}\\&=\left\{\frac{n_\alpha\alpha_0+2m_\beta\beta_0+m_\kappa\kappa_0+n_\tau\tau_0}{3(\alpha_0+2\beta_0+\kappa_0+\tau_0)}\left[1-\frac{C_{12}}{C_{11}}\right]+\frac{2}{3}\frac{l_\beta\beta_0+2l_\kappa\kappa_0-l_\tau\tau_0}{\alpha_0+2\beta_0+\kappa_0+\tau_0}\left[1+\frac{2C_{12}}{C_{11}}\right]\right\}e_{xx}\omega_0(X) .\end{aligned} \tag{22}$$

Three conditions are needed to obtain l_β, l_κ, and l_τ. Two conditions are readily available from experiments: the LO/TO splitting at Γ with uniaxial stress along [001], as described by Eq. (21), and the LO/TO splitting at Γ with uniaxial stress along [111], as is described by Eq. (30) in Sec. II E. The third condition used here is the assumption that [001] biaxial strain shifts $\omega_{\rm LO}$ by the same amount at Γ and X. This assumption is reasonable because the *ab initio* calculation of Ref. 10 showed that biaxial strain in the (001) plane shifts $\omega_{\rm LO}$ by approximately the same amount from Γ to X. Equating Eqs. (20a) and (22) gives

$$\left\{-2\gamma_{\mathrm{LO,LA}}(X)\left[1-\frac{C_{12}}{C_{11}}\right]+\frac{2}{3}\frac{l_\beta\beta_0+2l_\kappa\kappa_0-l_\tau\tau_0}{\alpha_0+2\beta_0+\kappa_0+\tau_0}\left[1+\frac{2C_{12}}{C_{11}}\right]\right\}\omega_0(X)$$
$$=\left\{-2\gamma_{\mathrm{LO,TO}}(\Gamma)\left[1-\frac{C_{12}}{C_{11}}\right]+\frac{2}{3}\frac{2l_\beta\beta_0+2l_\kappa\kappa_0+l_\tau\tau_0}{\alpha_0+\beta_0+\kappa_0-\tau_0}\left[1+\frac{2C_{12}}{C_{11}}\right]\right\}\omega_0(\Gamma)\ . \quad (23)$$

l_β, l_κ, and l_τ are determined by using Eqs. (21), (23), and (30) for Si and Ge, and are listed in Table II. Figure 7(a) [Fig. 8(a)] plots the shifts in phonon frequencies along [001] for Si (Ge) pseudomorphically grown on Ge (Si) (001). For Si grown on Ge (001), the Si layer is subjected to a tensile strain, leading to a downward shift in phonon frequencies, while for Ge grown on Si(001), the Ge layer is subjected to a compressive strain, leading to an upward shift in phonon frequencies. In both strained Si and Ge, $\Delta\omega_{\mathrm{LO}}$ remains almost constant throughout the zone, which is consistent with the observation in Ref. 10. The frequency shifts of the LO and LA modes for Si are similar to those calculated in Ref. 7, but the shifts of the TO and TA modes are quite different. $\Delta\omega_{\mathrm{TO}}$ decreases from -19 to -29 cm^{-1} from Γ to X, but increases from -22 to -12 cm^{-1} in Ref. 7. This difference is due, in part, to the increase in γ_{TO} from Γ to X, which is not reflected in Ref. 7 because their assumption of $n_\alpha=m_\beta$ leads to a constant γ_{TO}. From Γ to X, $\Delta\omega_{\mathrm{TA}}$ first increases slightly from 0 and then decreases to -53 cm^{-1} at X. In Ref. 7, $\Delta\omega_{\mathrm{TA}}$ decreases from 0 to -27 cm^{-1} nearly linearly from Γ to X. These general observations are also seen for strained Ge films.

Phonons in very thin films are affected by strain and also by confinement. A simple model based on standing waves explains the effect of confinement on LO phonons along Δ in (001) ultrathin layers, as in Si/Ge SLS's.[25] The effective wave vector for the standing wave is given by

$$q_{\mathrm{eff}}=\frac{s\pi}{d_0(t+\nu)}\ , \quad (24)$$

where s, d_0, and t are the number of half-wavelengths corresponding to the order of the mode, the thickness of one monolayer, and the number of monolayers, respectively. The parameter ν depends on detailed boundary conditions, and is 0 and 1 for low order modes in Si and Ge, respectively.[25] Only odd order modes are Raman active due to symmetry.

The frequency of confined LO phonons in (001) Si/Ge SLS's is $\omega_{\mathrm{bulk,LO}}(q_{\mathrm{eff}})+\Delta\omega_{\mathrm{LO}}(q_{\mathrm{eff}})$, where the second term gives the effect of strain. $\Delta\omega_{\mathrm{LO}}(q_{\mathrm{eff}})$ is almost dispersionless from Γ to X, which is due mostly to the assumption that $\Delta\omega_{\mathrm{LO}}(\Gamma)=\Delta\omega_{\mathrm{LO}}(X)$.

E. Biaxial strain in the (111) plane

Since the macroscopic strain e_{ij} does not uniquely define the relative positions of the atoms when biaxial strain is in the (111) plane, an additional parameter, the internal strain parameter ξ defined in Eq. (4), is needed. The strain parameter is determined by using Eq. (10e) and α_0, β_0, κ_0, and τ_0 from Table II. This gives $\xi=0.58$ for Si and 0.60 for Ge, which are very close to the experimental values 0.54 ± 0.04 for both c-Si and c-Ge.[26]

With biaxial strain in the (111) plane, the elements of the strain tensor are

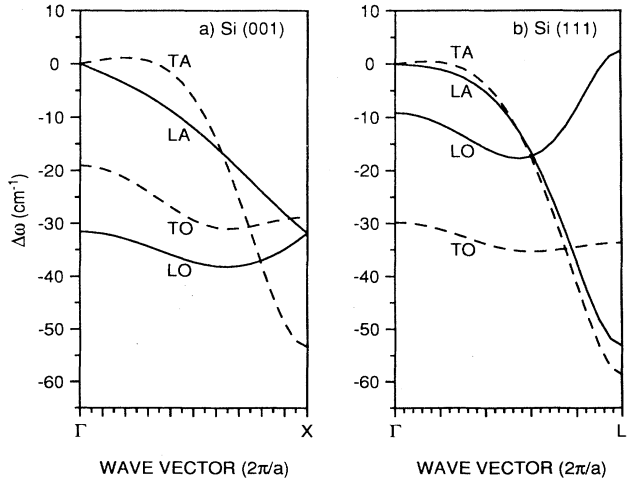

FIG. 7. Phonon frequency shifts $\Delta\omega$ along the growth direction in strained Si grown on (a) Ge (001) and (b) Ge (111), respectively. The solid lines and dashed lines represent longitudinal and transverse phonons, respectively.

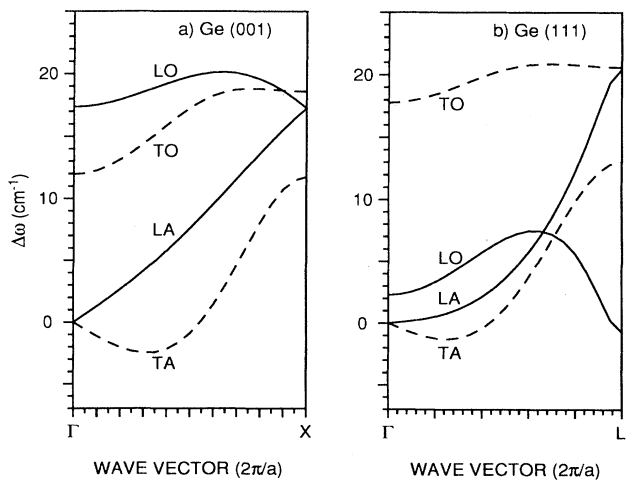

FIG. 8. Phonon frequency shifts $\Delta\omega$ along the growth direction in strained Ge grown on (a) Si (001) and (b) Si (111), respectively. The solid lines and dashed lines represent longitudinal and transverse phonons, respectively.

$$e^d=\frac{2C_{44}}{2C_{44}+C_{11}+2C_{12}}e_{\parallel}\ , \tag{25a}$$

$$e^0=-\frac{(C_{11}+2C_{12})}{2C_{44}+C_{11}+2C_{12}}e_{\parallel}\ , \tag{25b}$$

where $e^d=e_{xx}=e_{yy}=e_{zz}$ is the diagonal matrix element of the strain tensor, $e^0=e_{xy}=e_{yz}=e_{xz}$ is the off-diagonal matrix element, and $e_{\parallel}$ is the in-plane lattice mismatch strain which is $\sim 4\%$ for Ge pseudomorphically grown on Si.

Using Eq. (4), (111) strain changes the bond length parameter by

$$\Delta r\begin{bmatrix}0&0\\ \beta&\eta\end{bmatrix}=r_0(e^d+\sigma)\ , \tag{26a}$$

$$\Delta r\begin{bmatrix}0&1\\ \beta&\eta\end{bmatrix}=\Delta r\begin{bmatrix}0&2\\ \beta&\eta\end{bmatrix}=\Delta r\begin{bmatrix}0&3\\ \beta&\eta\end{bmatrix}=r_0(e^d-\tfrac{1}{3}\sigma)\ , \tag{26b}$$

where $\sigma=e^0(1-\xi)$. The changes in bond angle are

$$\Delta\theta\begin{bmatrix}0&0&-1\\ \beta&\eta&\beta\end{bmatrix}=\Delta\theta\begin{bmatrix}0&0&-2\\ \beta&\eta&\beta\end{bmatrix}=\Delta\theta\begin{bmatrix}0&0&-3\\ \beta&\eta&\beta\end{bmatrix}=\Delta\theta\begin{bmatrix}0&0&1\\ \eta&\beta&\eta\end{bmatrix}$$
$$=\Delta\theta\begin{bmatrix}0&0&2\\ \eta&\beta&\eta\end{bmatrix}=\Delta\theta\begin{bmatrix}0&0&3\\ \eta&\beta&\eta\end{bmatrix}=\frac{2e^0(1+2\xi)}{3\sqrt{2}}\ , \tag{27a}$$

$$\Delta\theta\begin{bmatrix}-1&0&-2\\ \beta&\eta&\beta\end{bmatrix}=\Delta\theta\begin{bmatrix}-1&0&-3\\ \beta&\eta&\beta\end{bmatrix}=\Delta\theta\begin{bmatrix}-2&0&-3\\ \beta&\eta&\beta\end{bmatrix}=\Delta\theta\begin{bmatrix}1&0&2\\ \eta&\beta&\eta\end{bmatrix}$$
$$=\Delta\theta\begin{bmatrix}1&0&3\\ \eta&\beta&\eta\end{bmatrix}=\Delta\theta\begin{bmatrix}2&0&3\\ \eta&\beta&\eta\end{bmatrix}=-\frac{2e^0(1+2\xi)}{3\sqrt{2}}\ . \tag{27b}$$

Therefore, using Eqs. (8a)–(8d), the corresponding quasiharmonic force constants for mismatch strain in the (111) plane are

$$\alpha_1=\alpha_0(1+n_\alpha e^d+n_\alpha\sigma)\ , \tag{28a}$$

$$\alpha_2=\alpha_0(1+n_\alpha e^d-\tfrac{1}{3}n_\alpha\sigma)\ , \tag{28b}$$

$$\beta_1=\beta_0(1+m_\beta e^d+\tfrac{1}{3}m_\beta\sigma+l_\beta\rho)\ , \tag{28c}$$

$$\beta_2=\beta_0(1+m_\beta e^d-\tfrac{1}{3}m_\beta\sigma-l_\beta\rho)\ , \tag{28d}$$

$$\kappa_1=\kappa_0(1+m_\kappa e^d+\tfrac{1}{3}m_\kappa\sigma+l_\kappa\rho)\ , \tag{28e}$$

$$\kappa_2=\kappa_0(1+m_\kappa e^d-\tfrac{1}{3}m_\kappa\sigma-l_\kappa\rho)\ , \tag{28f}$$

$$\tau_1=\tau_0(1+n_\tau e^d+\tfrac{1}{3}n_\tau\sigma+l_\tau\rho)\ , \tag{28g}$$

$$\tau_2=\tau_0(1+n_\tau e^d-\tfrac{1}{3}n_\tau\sigma-l_\tau\rho)\ , \tag{28h}$$

where $\rho=\frac{4}{3}e^0(1+2\xi)$.

The zone-center optical-phonon frequencies are

$$\omega_{\mathrm{LO}}(\Gamma)=\left[\frac{6\alpha_1+2\alpha_2+4(\beta_1+\beta_2)+4(\kappa_1+\kappa_2)-12\tau_1+4\tau_2}{M}\right]^{1/2}\ , \tag{29a}$$

$$\omega_{\mathrm{TO}}(\Gamma)=\left[\frac{8\alpha_2+4(\beta_1+\beta_2)+4(\kappa_1+\kappa_2)-8\tau_2}{M}\right]^{1/2}\ . \tag{29b}$$

The frequency splitting between the LO singlet and TO doublet is

$$\Delta\omega(\Gamma)=\omega_{\mathrm{LO}}(\Gamma)-\omega_{\mathrm{TO}}(\Gamma)$$
$$=\left[\frac{(n_\alpha\alpha_0-n_\tau\tau_0)\sigma-3l_\tau\tau_0\rho}{2(\alpha_0+\beta_0+\kappa_0-\tau_0)}\right]\omega_0(\Gamma)\ . \tag{30}$$

In Sec. III it will be seen that the term in brackets can be expressed as $3r/2\omega_0^2(\Gamma)$, where r is a parameter defined in Sec. III and Ref. 8. $r/\omega_0^2(\Gamma)$ has been measured to be -0.65 ± 0.13 for Si and -0.87 ± 0.09 for Ge.

Figure 7(b) [Fig. 8(b)] plots the shifts in phonon frequencies along [111] for Si (Ge) pseudomorphically grown on Ge (Si) (111). For Si grown on Ge (111), the Si layer is subjected to a tensile strain, leading to downward shifts in phonon frequencies. $\Delta\omega_{\mathrm{TO}}$ is almost constant along the growth direction, $-30\ \mathrm{cm}^{-1}$ at the Γ point and $-33\ \mathrm{cm}^{-1}$ at the L point. $\Delta\omega_{\mathrm{TA}}$ becomes positive (yet

small) near the Γ point and decreases to -59 cm^{-1} at the L point. $\Delta\omega_{LO}(L)$ and $\Delta\omega_{LA}(L)$ are $+2.5$ and -53 cm^{-1}, respectively. Similar behavior is observed for $\Delta\omega$ along [111] for Ge grown on Si (111).

F. Strained films and heterostructures under hydrostatic pressure

At ambient pressure, the magnitude of the lattice mismatch is $\sim 4\%$ for Ge grown pseudomorphically on Si(001) and vice versa, and $\sim 2\%$ for growth on $Si_{0.5}Ge_{0.5}$. The hydrostatic component of strain is

$$e_{ii}^{h}=\frac{\Delta r}{r_0}=-\frac{P}{3B}+\frac{2}{3}\left[1-\frac{C_{12}}{C_{11}}\right]e_{xx} \quad (i=x,y,z) , \tag{31}$$

where e_{xx} is the pressure-dependent in-plane lattice-mismatch strain assuming Ge grown on Si(001), which is defined as

$$e_{xx}(P)=\frac{a_{Si}(P)-a_{Ge}(P)}{a_{Ge}(P)} , \tag{32}$$

and C_{11} and C_{12} are the elastic constants of the strained Ge layer. These expressions, as well as those that follow, are explicitly written for strained Ge layers on Si. The traceless uniaxial components of strain are given in Eq. (17b). The effect of pressure on phonons in ultrathin strained layers and SLS's can be determined from the pressure response at q_{eff} for biaxially strained "thick" films.

Hydrostatic pressure tunes the biaxial strain through Eq. (32), which to first order in applied pressure changes as

$$e_{xx}(P)=e_{xx}(0)+\frac{a_{Si}(0)}{a_{Ge}(0)}\left[\frac{1}{3B_{Ge}}-\frac{1}{3B_{Si}}\right]P , \tag{33}$$

where

$$e_{xx}(0)=\frac{a_{Si}(0)-a_{Ge}(0)}{a_{Ge}(0)} \tag{34}$$

is the initial biaxial strain in the Ge film at ambient pressure ("$P=0$" corresponds to 1 bar).

The pressure derivative of the phonon frequencies can be expressed as

$$\frac{d\omega}{dP}=\frac{\partial\omega(e_{xx}(P),P)}{\partial P}+\frac{\partial\omega(e_{xx}(P),P)}{\partial e_{xx}(P)}\frac{de_{xx}(P)}{dP} , \tag{35}$$

where the first term on the right is due to the isotropic strain and the second is due to the pressure tuning of the mismatch strain. For very small P, Eq. (35) can be written as

$$\frac{d\omega}{dP}=\frac{\omega(e^{(b)},P)-\omega(e_0^{(b)},0)}{P} . \tag{36}$$

Using Eq. (35) or Eq. (36), $d\omega/dP$ at the zone center is approximately

$$\frac{d\omega_{LO}(P)}{dP}=\gamma_{LO,TO}(\Gamma)\frac{\omega_0}{B_{Ge}}+\left\{-2\gamma_{LO,TO}(\Gamma)\left[1-\frac{C_{12}}{C_{11}}\right]+\frac{2}{3}\frac{2l_\beta\beta_0+2l_\kappa\kappa_0+l_\tau\tau_0}{\alpha_0+\beta_0+\kappa_0-\tau_0}\left[1+\frac{2C_{12}}{C_{11}}\right]\right\}\left[\frac{1}{3B_{Ge}}-\frac{1}{3B_{Si}}\right]\omega_0 , \tag{37a}$$

$$\frac{d\omega_{TO}(P)}{dP}=\gamma_{LO,TO}(\Gamma)\frac{\omega_0}{B_{Ge}}+\left\{-2\gamma_{LO,TO}(\Gamma)\left[1-\frac{C_{12}}{C_{11}}\right]-\frac{2}{3}\frac{l_\beta\beta_0+l_\kappa\kappa_0+2l_\tau\tau_0}{\alpha_0+\beta_0+\kappa_0-\tau_0}\left[1+\frac{2C_{12}}{C_{11}}\right]\right\}\left[\frac{1}{3B_{Ge}}-\frac{1}{3B_{Si}}\right]\omega_0 , \tag{37b}$$

which is consistent with the calculations in Ref. 5.

The first terms on the right-hand sides of Eqs. (37a) and (37b) describe the effect of hydrostatic pressure on bulk Ge. The second term describes the tuning of biaxial strain in the Ge layer by the applied pressure. These results are easily extended to Ge grown on Si (111) and Si grown on Ge (001) or (111).

Figure 9 compares $d\omega/dP$ for phonons in a strained layer of Si on Ge(001) and (111) to that for unstrained Si. Figure 10 makes a similar comparison for strained Ge on Si (001) and (111) with unstrained Ge. The changes in the LO- and TO- phonon frequencies at zone center due to pressure are obtained from Eqs. (37a) and (37b). For both Si and Ge, the strain-induced perturbation to $d\omega/dP$ is almost constant from Γ to X for LO and TO phonons. Also, the changes in the LO- and LA-phonon frequencies are the same at the X point for both Si and Ge, as is expected from symmetry. Note that $d\omega/dP$ for LO and TO phonons in Si cross at about 0.3 ($2\pi/a$), while for Ge and for unstrained Si they do not cross.

Figure 10 also shows that the model agrees with the experimental pressure dependence of ω_{LO} for phonons confined in the Ge layers of a $Si_{12}Ge_4$ strained-layer superlattice.[5]

III. RELATING p, q, and r TO THE MODEL PARAMETERS

Cerdeira *et al.*[8] examined how strain changes the frequency of near-zone-center optical phonons in crystals with diamond structure by using the microscopically averaged spring constant parameters p, q, and r. The

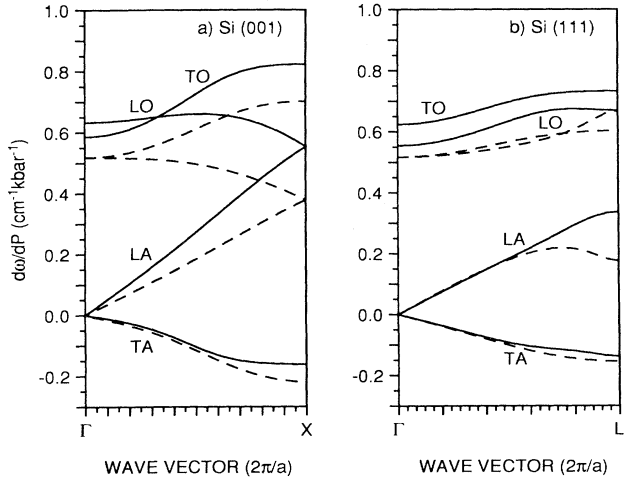

FIG. 9. $d\omega/dP$ for phonons along the growth direction in Si. The dashed lines represent Si with no biaxial strain, while the solid lines correspond to biaxially strained Si grown pseudomorphically on (a) Ge (001) and (b) Ge (111), respectively.

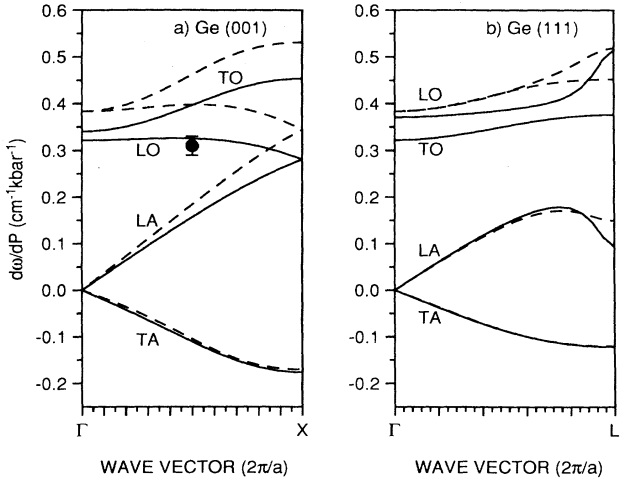

FIG. 10. $d\omega/dP$ for phonons along the growth direction in Ge. The dashed lines represent Ge with no biaxial strain, while the solid lines correspond to biaxially strained Ge grown pseudomorphically on (a) Si (001) and (b) (111), respectively. The solid dot is from Raman scattering of phonons that are quasiconfined in the strained Ge films of a $Si_{12}Ge_4$ SLS on c-Si (Ref. 5).

dynamical equation describing optical phonons is

$$m\ddot{u}_i = -K_{ii}^{(0)}u_i - \sum_{jkl} K_{ijkl}^{(1)} e_{kl} u_j \ , \tag{38}$$

where u is the dynamic displacement coordinate, m is the reduced mass of the two atoms in the unit cell, e_{kl} is the static strain, $K_{ii}^{(0)} = m\omega_0^2$, where ω_0 is the zone-center optical-phonon frequency in the absence of strain, $K_{ijkl}^{(1)} = \partial K_{ij}/\partial e_{kl}$, and i, j, k, and $l = x$, y, or z. Because of cubic symmetry, only three parameters are needed to describe the effect of strain: $p = K_{iiii}^{(1)}/m$, $q = K_{iijj}^{(1)}/m$, and $r = K_{ijij}^{(1)}/m$.

The strain-modified zone-center optical-phonon frequencies Ω are given by

$$\begin{vmatrix} pe_{xx}+q(e_{yy}+e_{zz})-\lambda & re_{xy} & re_{xz} \\ re_{yx} & pe_{yy}+q(e_{xx}+e_{zz})-\lambda & re_{yz} \\ re_{zx} & re_{zy} & pe_{zz}+q(e_{xx}+e_{yy})-\lambda \end{vmatrix} = 0 \ , \tag{39}$$

where $\lambda = \Omega^2 - \omega_0^2$.

With isotropic strain, one finds $\gamma_{\mathrm{LO,TO}}(\Gamma) = -(p+2q)/6\omega_0^2$. For biaxial strain in either the (001) or (111) plane, the threefold degenerate zone-center phonon is split into a singlet (Ω_s) with eigenvector perpendicular to the plane and a doublet (Ω_d) with eigenvectors parallel to the plane. Equation (39) gives

$$\Omega_s = \omega_0 + \Delta\Omega_H + \tfrac{2}{3}\Delta\Omega \ , \tag{40a}$$

$$\Omega_d = \omega_0 + \Delta\Omega_H - \tfrac{1}{3}\Delta\Omega \ . \tag{40b}$$

For biaxial strain in the (001) plane

$$\Delta\Omega_H = \frac{1}{3\omega_0}(p+2q)\left[1-\frac{C_{12}}{C_{11}}\right]e_{xx} \ , \tag{41a}$$

$$\Delta\Omega = \Omega_s - \Omega_d = -\frac{1}{2\omega_0}(p-q)\left[1+\frac{2C_{12}}{C_{11}}\right]e_{xx} \ , \tag{41b}$$

while for biaxial strain in the (111) plane

$$\Delta\Omega_H = \frac{1}{2\omega_0}(p+2q)e^d \ , \tag{42a}$$

$$\Delta\Omega = \Omega_s - \Omega_d = \frac{3r}{2\omega_0}e^0 \ . \tag{42b}$$

Similar splittings are seen in Secs. II D and II E. By comparing these expressions with Eqs. (15a), (20a), (20b), (21), and (30), p, q, and r are seen to be related to the current model parameters as

$$\frac{p+2q}{6\omega_0^2} = \frac{n_\alpha\alpha_0 + m_\beta\beta_0 + m_\kappa\kappa_0 - n_\tau\tau_0}{6(\alpha_0+\beta_0+\kappa_0-\tau_0)} \ , \tag{43a}$$

$$\frac{p-q}{2\omega_0^2} = -\frac{2(l_\beta\beta_0 + l_\kappa\kappa_0 + l_\tau\tau_0)}{\alpha_0+\beta_0+\kappa_0-\tau_0} \ , \tag{43b}$$

$$\frac{r}{\omega_0^2} = \frac{(n_\alpha\alpha_0 - n_\tau\tau_0)(1-\xi) - 4(1+2\xi)l_\tau\tau_0}{3(\alpha_0+\beta_0+\kappa_0-\tau_0)} \ . \tag{43c}$$

IV. RELATION OF STRAIN-MODIFIED FORCE CONSTANTS TO ANHARMONICITY

The adoption of strain-modified force constants can be justified by examining the effect of cubic terms in the potential. The anharmonic perturbation to the potential energy U' is

$$\begin{aligned}U'=&\tfrac{1}{6}\sum_{l}\sum_{i=1}^{4}\alpha'\Delta r^3\begin{bmatrix}l\\i\end{bmatrix}+\tfrac{1}{6}\sum_{l}\sum_{ji}\beta'\Delta\theta^3\begin{bmatrix}l\\ij\end{bmatrix}\\&+\tfrac{1}{6}\sum_{ll}\sum_{jin}\kappa'\Delta\theta^2\begin{bmatrix}l\\ij\end{bmatrix}\Delta\theta\begin{bmatrix}l'\\jn\end{bmatrix}+\tfrac{1}{6}\sum_{ll'}\sum_{ji}\tau'\Delta r^2\begin{bmatrix}l\\i\end{bmatrix}\Delta r\begin{bmatrix}l'\\j\end{bmatrix}+\tfrac{1}{6}\sum_{ll'}\sum_{ji}\delta_1'\Delta r\begin{bmatrix}l\\i\end{bmatrix}\Delta\theta^2\begin{bmatrix}l\\ij\end{bmatrix}\\&+\tfrac{1}{6}\sum_{ll'l''}\sum_{jin}\delta_2'\Delta\theta\begin{bmatrix}l\\ij\end{bmatrix}\Delta\theta\begin{bmatrix}l'\\jn\end{bmatrix}\left\{\Delta r\begin{bmatrix}l\\i\end{bmatrix}+2\Delta r\begin{bmatrix}l''\\j\end{bmatrix}+\Delta r\begin{bmatrix}l'\\n\end{bmatrix}\right\}\\&+\tfrac{1}{6}\sum_{ll'}\sum_{ji}\delta_3'\Delta\theta\begin{bmatrix}l\\ij\end{bmatrix}\Delta r\begin{bmatrix}l\\i\end{bmatrix}\Delta r\begin{bmatrix}l\\j\end{bmatrix}+\tfrac{1}{6}\sum_{ll'}\sum_{ji}\delta_4'\Delta r^2\begin{bmatrix}l\\i\end{bmatrix}\Delta\theta\begin{bmatrix}l\\ij\end{bmatrix},\end{aligned}\tag{44}$$

where only the third-order terms diagramed in Fig. 11 are included. (For clarity, $(\Delta r[{}^{l}_{i}])^3$ has been written as $\Delta r^3[{}^{l}_{i}]$, etc.) Other third-order terms are assumed to be small. All energies and parameters involving the cubic terms are primed.

The third-order static contribution U_0' and dynamic contribution U_2' are found by inserting Eq. (3) in Eq. (44). Adding U_2' to U_2, the quasiharmonic force constants are seen to be

$$\alpha_i=\alpha_0+\tfrac{1}{2}\alpha'\Delta r_s\begin{bmatrix}l\\i\end{bmatrix}+\tfrac{1}{6}\sum_{l'}\sum_{j\neq i}\tau'\Delta r_s\begin{bmatrix}l'\\j\end{bmatrix}+\tfrac{1}{6}\sum_{l'}\sum_{j\neq i}\delta_4'\Delta\theta_s\begin{bmatrix}l\\ij\end{bmatrix},\tag{45a}$$

$$\beta_{ij}=\beta_0+\tfrac{1}{2}\beta'\Delta\theta_s\begin{bmatrix}l\\ij\end{bmatrix}+\tfrac{1}{6}\sum_{l'l''}\sum_{n}\kappa'\Delta\theta_s\begin{bmatrix}l'\\jn\end{bmatrix}+\tfrac{1}{6}\delta_1'\Delta r_s\begin{bmatrix}l'\\i\end{bmatrix}+\tfrac{1}{6}\delta_1'\Delta r_s\begin{bmatrix}l''\\j\end{bmatrix},\tag{45b}$$

$$\begin{aligned}\kappa_{ijk}=&\kappa_0+\tfrac{1}{3}\kappa'\Delta\theta_s\begin{bmatrix}l\\ij\end{bmatrix}+\tfrac{1}{3}\kappa'\Delta\theta_s\begin{bmatrix}l\\jk\end{bmatrix}\\&+\tfrac{1}{6}\delta_2'\left\{\Delta r_s\begin{bmatrix}l'\\i\end{bmatrix}+2\Delta r_s\begin{bmatrix}l''\\j\end{bmatrix}+\Delta r_s\begin{bmatrix}l'''\\k\end{bmatrix}\right\},\end{aligned}\tag{45c}$$

$$\tau_{ij}=\tau_0+\tfrac{1}{6}\delta_3'\Delta\theta_s\begin{bmatrix}l\\ij\end{bmatrix}+\tfrac{1}{3}\tau'\Delta r_s\begin{bmatrix}l'\\i\end{bmatrix}+\tfrac{1}{3}\tau'\Delta r_s\begin{bmatrix}l''\\j\end{bmatrix}.\tag{45d}$$

The summations involving τ' and δ_4' in Eq. (45a) are ignored since α' is one order of magnitude larger than τ' and δ_4'. (This condition leads to $\delta_4'=0$.) The summation involving κ' in Eq. (45b) is also expected to give a negligible contribution.

The change in the "Keating" bond-stretching coordinate $\Delta r_s({}^{l}_{i})$ and the bond-bending coordinate $\Delta\theta_s({}^{l}_{ij})$ due to static displacements [Eqs. (2a) and (2b) with $\Delta\tilde{\mathbf{u}}({}^{l}_{i})$ replaced by $\Delta\mathbf{u}_s({}^{l}_{i})$] can also be expressed as

$$\Delta r_s\begin{bmatrix}l\\i\end{bmatrix}=\frac{\mathbf{r}\begin{bmatrix}l\\i\end{bmatrix}\cdot\Delta\mathbf{u}_s\begin{bmatrix}l\\i\end{bmatrix}}{a'},\tag{46a}$$

$$\Delta\theta_s\begin{bmatrix}l\\ij\end{bmatrix}=\frac{1}{2a'}\left\{\mathbf{r}\begin{bmatrix}l\\i\end{bmatrix}\cdot\Delta\mathbf{u}_s\begin{bmatrix}l\\j\end{bmatrix}+\mathbf{r}\begin{bmatrix}l\\j\end{bmatrix}\cdot\Delta\mathbf{u}_s\begin{bmatrix}l\\i\end{bmatrix}\right\}.\tag{46b}$$

To first order, they can be related to the actual changes in bond length Δr_i and bond angle $\Delta\theta_{ij}$ by

$$\Delta r_s\begin{bmatrix}l\\i\end{bmatrix}=\sqrt{3}\Delta r_i,\tag{47a}$$

$$\Delta\theta_s\begin{bmatrix}l\\ij\end{bmatrix}=-\frac{1}{2\sqrt{3}r_0}\Delta(r_ir_j)-\frac{\sqrt{2}}{\sqrt{3}}r_0\Delta\theta_{ij}.\tag{47b}$$

After inserting Eqs. (47a) and (47b) into Eqs. (45a)–(45d), and comparing with Eqs. (8a)–(8d), it is seen that

$$\alpha'=\frac{2}{\sqrt{3}r_0}n_\alpha\alpha_0,\tag{48a}$$

$$\beta'=-\frac{4\sqrt{3}}{r_0}l_\beta\beta_0,\tag{48b}$$

$$\kappa'=-\frac{3\sqrt{3}}{r_0}l_\kappa\kappa_0,\tag{48c}$$

$$\tau'=\frac{\sqrt{3}}{2r_0}(n_\tau-2l_\tau)\tau_0 , \tag{48d}$$

$$\delta_1'=\frac{\sqrt{3}}{r_0}(m_\beta-2l_\beta)\beta_0 , \tag{48e}$$

$$\delta_2'=\frac{\sqrt{3}}{2r_0}(m_\kappa-2l_\kappa)\kappa_0 , \tag{48f}$$

$$\delta_3'=-\frac{12\sqrt{3}}{r_0}l_\tau\tau_0 . \tag{48g}$$

This analysis shows why the parameters n_α, m_β, m_κ, and n_τ that describe the quasiharmonic force constants must have different values, in contrast to earlier assumptions.[7,8,11]

V. DERIVATION OF ELASTIC CONSTANTS USING STRAIN-MODIFIED FORCE CONSTANTS

The second-order elastic constants are given by Eqs. (10a)–(10e) with α_0, β_0, κ_0, and τ_0 replacing α, β, κ, and τ, respectively. The third-order elastic constants[27] are obtained by comparing the macroscopic third-order strain energy density U_0'/V defined as

$$\begin{aligned}\frac{U_0'}{V}=&\tfrac{1}{6}(C_{111}+3C_{11})(e_{xx}^3+e_{yy}^3+e_{zz}^3)+C_{123}e_{xx}e_{yy}e_{zz}\\&+\tfrac{1}{2}(C_{112}+C_{12})\{e_{xx}^2(e_{yy}+e_{zz})+e_{yy}^2(e_{xx}+e_{zz})+e_{zz}^2(e_{xx}+e_{yy})\}\\&+\tfrac{1}{2}C_{144}\{e_{xx}e_{yz}^2+e_{yy}e_{xz}^2+e_{zz}e_{xy}^2\}\\&+\tfrac{1}{2}C_{166}\{e_{xx}(e_{xy}^2+e_{xz}^2)+e_{yy}(e_{xy}^2+e_{yz}^2)+e_{zz}(e_{yz}^2+e_{xz}^2)\}+\tfrac{1}{2}C_{456}e_{xy}e_{xz}e_{yz}\end{aligned} \tag{49}$$

with the third-order microscopic static strain energy defined in Eq. (44). This leads to

$$C_{111}=\frac{\alpha'}{4}-\frac{\beta'}{4}-\frac{\kappa'}{4}+\frac{3\tau'}{2}+\frac{3\delta_1'}{2}+3\delta_2'-\frac{\delta_3'}{4}-3C_{11} , \tag{50a}$$

$$C_{112}=\frac{\alpha'}{4}-\frac{\beta'}{4}-\frac{\kappa'}{4}+\frac{3\tau'}{2}+\frac{\delta_1'}{6}+\frac{\delta_2'}{3}-\frac{\delta_3'}{4}-C_{12} , \tag{50b}$$

$$C_{123}=\frac{\alpha'}{4}+\frac{3\beta'}{4}+\frac{3\kappa'}{4}+\frac{3\tau'}{2}-\frac{\delta_1'}{2}-\delta_2'-\frac{\delta_3'}{4} , \tag{50c}$$

$$C_{144}=\frac{(1-\xi)^2}{4}\alpha'+\frac{(1+\xi)^2}{4}\beta'+\frac{(1+\xi)^2}{4}\kappa'+\frac{(1-\xi)^2}{2}\tau'+\frac{3\xi^2+2\xi-1}{12}\delta_1'+\frac{3\xi^2+2\xi-1}{6}\delta_2'+\frac{(1-\xi)^2}{2}\delta_3' , \tag{50d}$$

$$C_{166}=\frac{(1-\xi)^2}{4}\alpha'-\frac{(1+\xi)^2}{4}\beta'-\frac{(1+\xi)^2}{4}\kappa'+\frac{(1-\xi)^2}{2}\tau'+\frac{3+2\xi-\xi^2}{12}\delta_1'-\frac{3+2\xi-\xi^2}{6}\delta_2'-\frac{(1-\xi)^2}{6}\delta_3' , \tag{50e}$$

$$C_{456}=\frac{(1-\xi)^3}{4}\alpha'-\frac{(1-\xi)^3}{2}\tau'+\frac{(1-\xi)^2(1+\xi)}{2}\delta_3' , \tag{50f}$$

where C_{11} and C_{12} are given by Eqs. (10a) and (10b).

The two-parameter Keating model[19,27] and the current model both describe the second- and third-order elastic constants very well when the model parameters are fit only to the elastic constant data. However, the second-order elastic constants for Si and Ge predicted by the model do not agree well with experiment when the harmonic force constants in Table II, which were optimized for phonons, are used in Eqs. (10a)–(10e) (see Table IV). To improve the fit to all available data, α_0, β_0, κ_0, and τ_0 were also obtained by optimizing to both the phonon dispersion and the elastic constants C_{11}, C_{12}, and C_{44}, with comparable average deviations, giving $\alpha_0=4.51$, $\beta_0=0.489$, $\kappa_0=0.914$, and $\tau_0=0.136$ (in units of 10^{12} dyn/cm) for Si, and $\alpha_0=3.78$, $\beta_0=0.424$, $\kappa_0=0.762$, and $\tau_0=0.049$ (in units of 10^{12} dyn/cm) for Ge, respectively. With these new values, the average error in the fit to phonon dispersion increases from 1.7% to 2.6% for Si and from 2.3% to 4.7% for Ge. The agreement with the elastic constants is now very good (Table IV). The current four-parameter model fits elastic constants and phonon data as well as does the four-parameter bond-charge[16] when these revised parameters are used, and it is superior to the two-parameter Keating model.

Note that κ_0 increases for both Si and Ge when the fits include the elastic constant data. Since κ_0 characterizes long-range interactions, which include up to the fifth-nearest-neighbor atoms, this increase in κ_0 indicates that the elastic force constants depend more strongly on long-range interactions than do optical phonons.

Similarly, the third-order elastic constants [Eqs. (50a)–(50f)] do not agree well with experiment[28] when the parameters in Table II, which were obtained from fits to γ_i, are used. Again, the fits can be improved by optimizing the seven primed parameters to the third-order elastic constants, the mode Grüneisen parameters at the critical points, and the splitting of zone-center optical-phonon frequencies under biaxial strain. This leads to -6.99, 8.01, -8.56, 2.35, -2.68, 0.01, and 0.37 for n_α, m_β, m_κ, n_τ, l_β, l_κ, and l_τ, respectively, for Si. The fit to the third-order elastic constants is improved, though not excellent, with the average deviation being $\sim$20%. The fit

TABLE IV. Structural parameters of Si and Ge used in the calculation and comparison of the second-order elastic constants.

	Si	Ge	unit
a_0	5.431[a]	5.657[a]	Å
C_{11}	1656[b]	1288[b]	kbar
	1848[c]	1566[c]	
	1679[d]	1322[d]	
C_{12}	639[b]	483[b]	kbar
	980[c]	873[c]	
	646[d]	484[d]	
C_{44}	795[b]	671[b]	kbar
	606[c]	482[c]	
	762[d]	629[d]	

[a]Reference 36.
[b]S. S. Mitra and N. E. Massa, in *Handbook on Semiconductors*, edited by T. S. Moss (North-Holland, Amsterdam, 1986), Vol. 1, p. 96.
[c]Fit using model parameters optimized to the phonon frequencies only.
[d]Fit using model parameters optimized to both the phonon frequencies and the elastic constants.

to the mode Grüneisen parameters is noticeably poorer. More cubic interactions, and perhaps also quartic interactions, must be included to obtain a good fit to all the data. Also, inclusion of the summations in Eqs. (45a) and (45b) may improve the fit. Still the current model provides a very good description of the effect of strain on phonons.

VI. DISCUSSION

This presented microscopic model is sufficiently detailed to describe the effects of strain on diamond-structure crystals. Isotropic strain affects only bond lengths, and biaxial strain in either the (001) or (111) plane affects both bond lengths and bond angles. The traceless components of the strain tensor for (001) strain affect only bond angles.

This model also describes phonons in strained-layer superlattices well, at ambient and elevated pressure. In Ref. 5 the effect of pressure on phonons confined in ultrathin layers in Si/Ge SLS's was expressed as the sum of three terms: those due to changes to phonons in the bulk, the changing strain, and the effect of confinement. Pressure-related changes of confinement were attributed to the differences in the mode Grüneisen parameter between phonons at zone center, as in the bulk, and phonons at q_{eff} from Eq. (24). All of these effects are implicitly included in Figs. 9 and 10 by considering phonons at the effective "folded" wave vector in the very thin, strained layer.

The coordinates used in this model have the better features of the Keating and valence-force-field potential coordinates. They are rotationally invariant, as are Keating coordinates and the valence coordinates. Like the Keating coordinates, they are easily transformed to Cartesian coordinates. For valence coordinates, this transformation is done with the rather cumbersome Wilson formula.[29] The current coordinates are linearly related to the bond distances and bond angles, while the Keating coordinates are nonlinearly related to them. Consequently, the harmonic Keating potential actually includes cubic terms that are usually ignored. Strain can be easily included into the current coordinates.

The inclusion of coplanar-angle (κ) and nearest bond-bond (τ) interactions, which are not in the original Keating model, is essential to this analysis. The κ interaction flattens the TA-phonon dispersion at ambient pressure. The τ interaction is needed to explain the $\omega_{\text{LO}}(\Gamma)/\omega_{\text{TO}}(\Gamma)$ splitting with biaxial strain in the (111) plane. Without this parameter, $r/\omega_0^2(\Gamma)$ [Eq. (43c)] cannot be modeled well at all.

The parameters in Table II were obtained using only phonon data and should be used when analyzing phonons in unstrained and strained crystals. When these parameters are revised to also fit elastic data, the fit to phonons is poorer. This is particularly significant in the analysis of the effect of strain through the cubic terms, where the fit does not satisfactorily model the third-order elastic constants and the dispersion of the mode Grüneisen parameters simultaneously. It should be relatively easy to obtain a physically plausible force-field model that fits all these data by including more interactions, particularly those that are even longer range than those considered

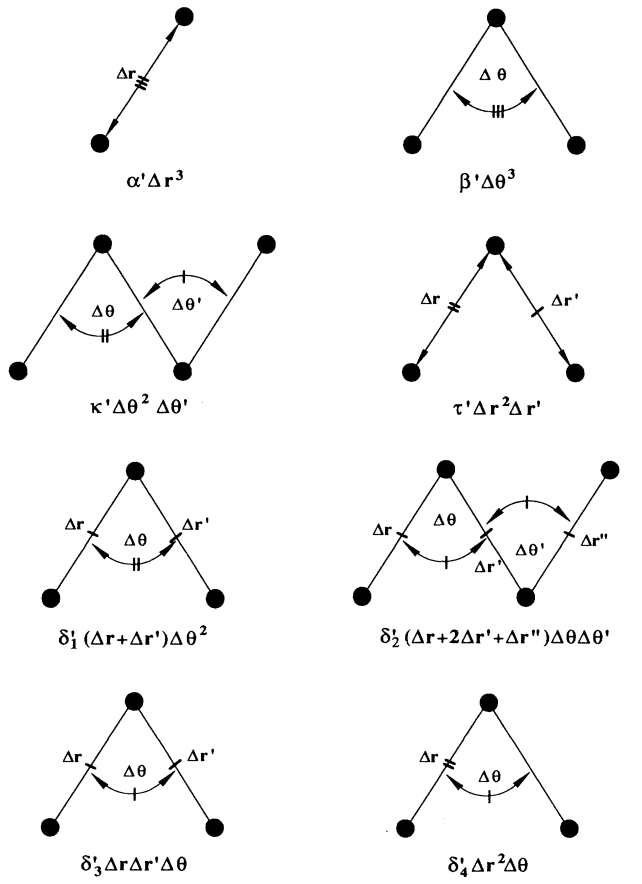

FIG. 11. Schematic representation of the cubic interactions included in Eq. (44).

here. The importance of such terms is not surprising. Sometimes quartic terms have been found to be as important as cubic terms in describing the lowest-order effects of temperature on optical phonons.[30–32]

A unique fit to the model requires the use of both phonon frequencies and eigenvectors. Since the eigenvectors (from *ab initio* calculations) are generally not available, only phonon frequencies were used here. Still, the parameters in Table II should be quite good because they predict phonon dispersions that are in agreement with *ab initio* calculations.

The negative values for n_α and n_τ derived in this study for *c*-Si and *c*-Ge imply that the bonds strengthen radially with the increase of the applied hydrostatic pressure. In contrast, the positive values of m_β and m_κ show that the force constants associated with the bond angle weaken with increased pressure. With further increase of pressure, the interaction between the bonds decreases so much that the diamond structure is no longer energetically favorable and a phase transition occurs. The phase transition for Si is $\sim$125 kbar (Ref. 22) and for Ge is $\sim$110 kbar.[23] A similar weakening of the bond-bending force constant with increasing hydrostatic pressure was found for HgSe by Ford *et al.*,[33] who used Martin's model[34] to describe this ionic crystal.

Lax[35] has made the important suggestion that the asymptotic behavior of the interatomic forces in diamond-type crystals is determined by quadrupole-quadrupole interactions, and such interactions have long-range character. Therefore, it is important to examine the convergence properties of this model. An important consequence of this long-range character is that the expressions for the second- and third-order elastic constants converge very slowly. For example, in Eq. (50a) the coefficient multiplying δ_2' is 12 times that for α', though δ_2' is almost an order of magnitude smaller than α'. Still, this model is fine for calculating the frequencies of optical phonons, for which short-range interactions are dominant, even under strain.

This model is able to express the parameters *p*, *q*, and *r* in terms of microscopic parameters. Previously, Ganesan, Maradudin, and Ottman[36] studied zone-center optical phonons in diamond structure materials. *p*, *q*, and *r* were determined by using only the bond-stretching forces [the first term in Eq. (1)], and did not agree with experiment. Cerdira *et al.*[8] examined the effect of strain on optical phonons at zone center using the Keating model, where *p*, *q*, and *r* were determined, and the VFF model, where only *p* and *q* were determined. The expression for *r* from the Keating model did not agree with experiment. *p* and *q* obtained from the VFF model did not agree with experiment when published model parameters were used. The authors did not try to optimize these model parameters. Bell[6] added anharmonic contributions to the strain energy and determined *p*, *q*, and *r* with the Keating model.

Some of the conclusions drawn in Refs. 7, 8, and 11 about phonon dispersion in strained Si and Ge layers at ambient pressure need to be altered because of their assumption about the scaling parameters for strain-modified force constants. The assumption of $n_\alpha = m_\beta$ in Refs. 7 and 8 implies that the mode Grüneisen parameter is the same regardless of phonon branch and wave vector. With this assumption, phonon dispersion cannot be correct when a crystal is under any type of strain that changes bond lengths. Reference 11 assumed that the force constants associated with bond angles are not affected by the presence of the strain. This study shows that this assumption is incorrect. Still, Refs. 7 and 11 correctly emphasized the need to use strain-modified force constants in analyzing strained heterostructures, such as Si/Ge superlattices. The current model provides a framework and data base for such calculations.

VII. CONCLUDING REMARKS

The dispersion relations for optical and acoustic phonons have been examined in bulk Si and Ge, Si and Ge strained layers grown on (001) and (111), and ultrathin Si/Ge superlattices at ambient pressure and under hydrostatic pressure by using a modified Keating model. Fits have been made using experimental data and several *ab initio* results, and there is good agreement with other experimental results, including those for superlattices. This model includes four interactions, which involve up to the fifth-nearest-neighbor atom, and force constants that depend on strain, the use of which is justified by analyzing cubic terms in the potential energy. In addition to specific calculations of phonon dispersion, analytic forms for the Grüneisen parameters at zone center and boundaries are obtained for bulk *c*-Si and *c*-Ge. For Si and Ge grown epitaxially on a (111) substrate, the frequency shift due to the biaxial strain for the TO-phonon mode is found to be almost independent of wave vector along [111]. The microscopically averaged empirical parameters *p*, *q*, and *r* that describe the effects of strain on optical phonons have been expressed in terms of our more microscopic model parameters. This model is also used to obtain the second- and third-order elastic constants for Si and Ge.

Phonons in diamond-structure crystals are described very well by this model. Further work can go in several directions. A more comprehensive treatment, including higher-order interactions, is needed to allow simultaneous fitting of all phonon data and third-order elastic constants in these crystals. With some modifications, this model can likewise be applied to III-V and II-VI zinc-blende materials, just as the original Keating model was extended in Ref. 34 to describe phonons in ionic crystals.

ACKNOWLEDGMENTS

The authors would like to thank M. Thompson, B. Weinstein, and R. Eryigit for helpful discussions and suggestions. This work was supported by the Joint Services Electronics Program under Contract No. DAAL03-91-C-0016.

[1]J. Bevk, A. Ourmazd, L. C. Feldman, T. P. Pearsall, J. M. Bonar, B. A. Davidson, and J. P. Mannaerts, Appl. Phys. Lett. **50**, 760 (1987).
[2]E. Kasper, H. Kibbel, H. Jorke, H. Brugger, E. Friess, and G. Abstreiter, Phys. Rev. B **38**, 3599 (1988).
[3]R. People and S. A. Jackson, Phys. Rev. B **36**, 1310 (1987).
[4]T. P. Pearsall, Crit. Rev. Solid State Mater. Sci. **15**, 551 (1989), and references cited therein.
[5]Z. Sui, I. P. Herman, and J. Bevk, Appl. Phys. Lett. **58**, 2351 (1991).
[6]M. I. Bell, Phys. Status Solidi B **53**, 675 (1972).
[7]J. Zi, K. Zhang, and X. Xie, Phys. Rev. B **45**, 9447 (1992).
[8]F. Cerdeira, C. J. Buchenauer, F. H. Pollak, and M. Cardona, Phys. Rev. B **5**, 580 (1972).
[9]P. Giannozzi, S. de Gironcoli, P. Pavone, and S. Baroni, Phys. Rev. B **43**, 7231 (1991).
[10]Q. Qteish and E. Molinari, Phys. Rev. B **42**, 7090 (1990).
[11]R. A. Ghanbari, J. D. White, G. Fasol, C. J. Gibbings, and C. G. Tuppen, Phys. Rev. B **42**, 7033 (1990).
[12]G. Dolling and R. A. Cowley, Proc. Phys. Soc. London **88**, 463 (1966).
[13]H. Jex, Phys. Status Solidi B **45**, 343 (1971).
[14]C. H. Xu, C. Z. Wang, C. T. Chan, and K. M. Ho, Phys. Rev. B **43**, 5024 (1991); also see D. N. Talwar and K. S. Suh, *ibid.* **36**, 6045 (1987).
[15]S. de Gironcoli, Phys. Rev. B **46**, 2412 (1992).
[16]W. Weber, Phys. Rev. B **15**, 4789 (1977).
[17]R. Tubino, L. Piseri, and G. Zerbi, J. Chem. Phys. **56**, 1022 (1972).
[18]H. L. McMurry, A. W. Solbrig, Jr., J. K. Boyter, and C. Noble, J. Phys. Chem. Solids **28**, 2359 (1967).
[19]P. N. Keating, Phys. Rev. **145**, 637 (1966).
[20]G. Dolling, *Inelastic Scattering of Neutrons in Solids and Liquids* (IAEA, Vienna, 1963), Vol. II, p. 37.
[21]G. Nilsson and G. Nelin, Phys. Rev. B **3**, 364 (1971).
[22]B. A. Weinstein and G. J. Piermarini, Phys. Rev. B **12**, 1172 (1975).
[23]D. Olego and M. Cardona, Phys. Rev. B **25**, 1151 (1981).
[24]R. T. Payne, Phys. Rev. Lett. **13**, 53 (1964).
[25]E. Friess, K. Eberl, U. Menczigar, and G. Abstreiter, Solid State Commun. **73**, 203 (1990).
[26]C. S. G. Cousins, L. Gerward, J. S. Olsen, B. Selsmark, and B. J. Sheldon, J. Phys. C **20**, 29 (1987).
[27]P. N. Keating, Phys. Rev. **149**, 674 (1966).
[28]H. J. McSkimin and P. Andreatch, Jr., J. Appl. Phys. **35**, 3312 (1964).
[29]E. B. Wilson, Jr., J. C. Decius, and P. C. Cross, in *Molecular Vibration* (McGraw-Hill, New York, 1955).
[30]H. Tang and I. P. Herman, Phys. Rev. B **43**, 2299 (1991).
[31]D. Vanderbilt, S. G. Louie, and M. L. Cohen, Phys. Rev. B **33**, 8740 (1986).
[32]E. Haro, M. Balkanski, R. F. Wallis, and K. H. Wanser, Phys. Rev. B **34**, 5358 (1986).
[33]P. J. Ford, A. J. Miller, G. A. Saunders, Y. K. Yogurtcu, J. K. Furdyna, and M. J. Jaczynski, J. Phys. C **15**, 657 (1982).
[34]R. M. Martin, Phys. Rev. B **1**, 4005 (1970).
[35]M. Lax, Phys. Rev. Lett. **1**, 133 (1958).
[36]S. Ganesen, A. A. Maradudin, and J. Ottmaa, Ann. Phys. **56**, 556 (1970).